DESIGN OF COMPOSITE FILTRATION MEDIA USING FLOW POROMETRY

Dr. Akshaya Jena and Dr. Krishna Gupta
Porous Materials, Inc.
83 Brown Road, Ithaca, NY 14850

Abstract

Filtration media are required to have suitable pore size, pore size distribution, pore volume, pore surface area and permeability for performing satisfactorily in applications. It is difficult to encounter all the desired properties in a filtration medium. In this investigation, we have characterized filtration media by flow porometry, used these pre-characterized filtration media to design composite filtration media, and tested these composites by flow porometry. Specimen of the filtration medium to be tested is soaked in a wetting liquid and gas pressure on one side of the specimen is slowly increased to displace the liquid from the pores and increase gas flow. Gas pressure and flow rates through wet and dry samples are measured and analyzed to obtain the largest pore size, the pore size distribution, and permeability. All of these characteristics of filtration media were measured in this investigation. It was shown that composite filtration media possessing unique characteristics could be prepared by a logical selection of pre-characterized filtration media.

INTRODUCTION

Nonwoven and woven filtration media are widely used in industry for separating suspended particles from fluids. The largest particle that cannot pass through the filter is determined by the largest pore diameter in the filter. The mean flow pore diameter and pore size distribution, determine sizes of other particles, which may not pass through. Permeability determines the rate of the filtration process. Therefore, all these properties need to be controlled in the filter. Control of such parameters is often difficult. However, it may be easier to produce controlled characteristics in composite filtration media prepared from filters with known characteristics.
In this investigation filtration media have been characterized. Composite filtration media have been prepared and characterized by flow porometry.. The results have been critically examined.

THE TECHNIQUE

Principle

A sample of the material to be tested is soaked in a wetting liquid. These liquids are such that the liquid/solid(filter) interfacial free energy is less than the gas/solid(filter) interfacial free energy. Therefore, the wetting liquid fills the pores spontaneously, but cannot be spontaneously removed from the pores. Gas under pressure is applied to one side of the sample, so that the work done by the gas in displacing the liquid inside the pore can compensate for the increase in free energy caused by the increase in gas/solid surface due to the displacement of the liquid in the pore. This is illustrated in Figure 1.

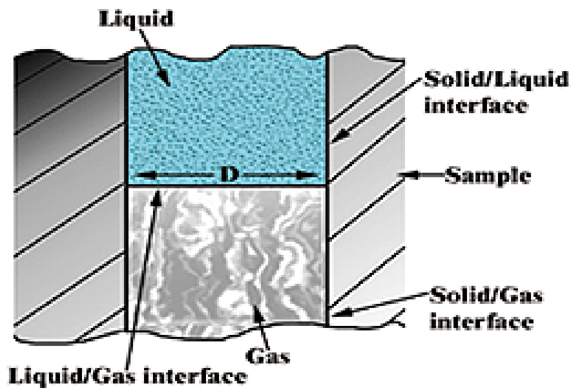

Figure 1. Displacement of liquid in a pore.

Free energy balance may be used to derive the pressure required to displace the liquid at any location in the pore [1]. The relation is given below.

$$p = \gamma \cos \theta \, (dS/dV) \qquad (1)$$

where,

p = differential pressure across the sample
γ = surface tension of the liquid
θ = contact angle
dS = increase in gas/solid surface area in the pore
dV = increase in volume of gas in the pore.

For a cylindrical pore of diameter D, (dS/dV) = (4/D). It follows from this relation that the largest pore will be emptied at the lowest pressure. When the gas pressure is increased, at a certain value of the pressure the largest pore is emptied and gas starts flowing through the sample. With further increase in pressure, gas removes liquid from smaller pores and the gas flow through the sample is increased. The differential gas pressure and the flow rates through wet and dry samples are measured. These data are used to calculate all the pore characteristics.

Equipment

The sample chamber is shown in Figure 2. It is so designed that the gas is allowed to escape only through the sample.

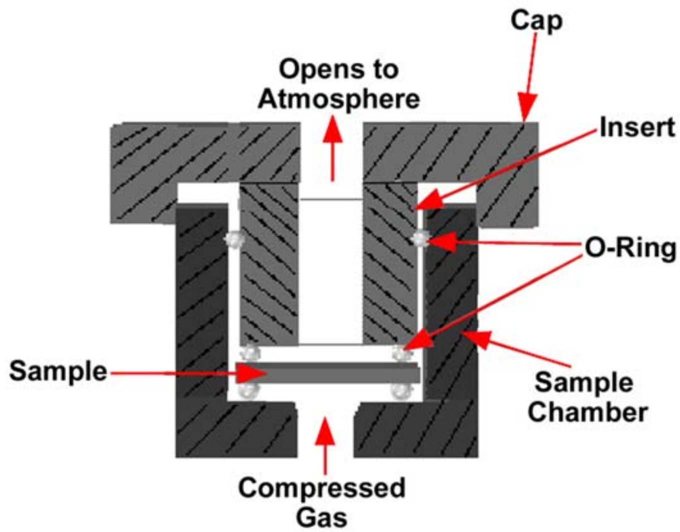

Figure 2. Sample chamber

The instrument used in this investigation, was equipped with state-of-the-art devices and innovative design for accurate control and sensing of pressure and flow. The instrument was fully automated using windows based software. It requires very little operator time and produces highly reproducible data [2]. The instrument is shown in Figure 3.

Figure 3. The Capillary Flow Porometer

RESULTS AND DISCUSSION

Pore diameter

The flow rate-pressure data for a filter material are shown in Figure 4. The dry curve in this figure refers to data obtained with a dry sample and the wet curve corresponds to the sample whose pores at the beginning of the test were filled with the wetting liquid.

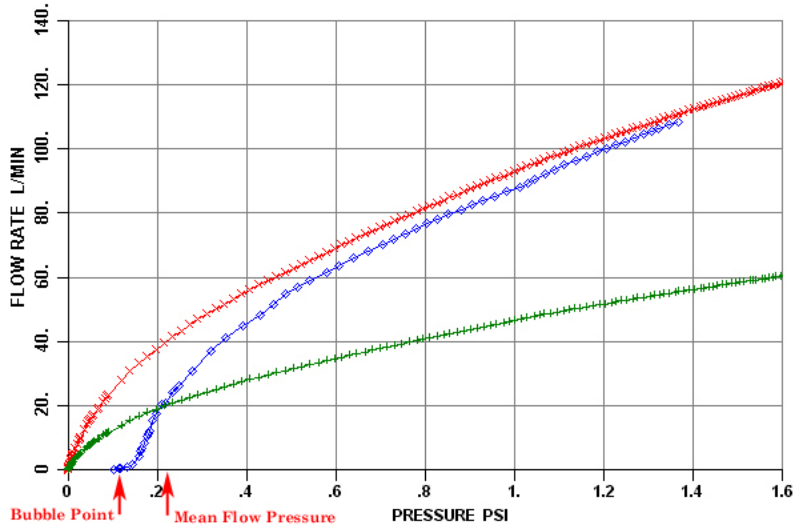

Figure 4. Variation of flow rate with pressure

The pore diameter is defined as the diameter D of a cylindrical opening such that (dS/dV) of the opening is the same as that of the pore at the location at which the gas displaces the liquid. For a cylindrical opening (dS/dV) is (4/D). Consequently, Equation 1 reduces to:

$$D = (4 \gamma \cos \theta) / p \qquad (2)$$

The wetting liquid Silwick was used. The surface tension of the liquid was 20.1 dynes/cm. Pore diameter was calculated taking cos θ to be one for this low surface tension wetting liquid [1].

The largest pore diameter (Bubble point)

The largest pore diameter corresponded to the pressure at which flow started (Figure 4). The bubble point pressure is shown in Figure 4.Six filter materials designated as 1, 2, 3, 4, 5 & 6, were investigated. A number of samples taken from each material were tested. The largest pore diameters found in the filters are listed in Table I. The bubble point pore diameters in the investigated filters are in the range of about 25 and 120 microns.

Table I. The largest pore diameter, mean flow pore diameter and permeability of six filter materials

	Filter #1	#2	#3	#4	#5	#6
The largest pore diameter, microns	120.6	25.17	24.29	86.54	61.53	96.07
Mean flow pore diameter, microns	40.45	11.73	11.77	43.67	23.20	44.77
Permeability, darcies	10.44	0.520	0.515	0.628	0.723	1.68

The mean flow pore diameter

The mean flow pore diameter corresponds to the pressure at which the wet curve and the half dry curve shown in Figure 4 intersect. The half dry curve is calculated from the dry curve so that at a given pressure the half dry curve gives half of the flow through the dry curve. Consequently, half of the flow through the dry sample is through pores having diameters greater than the mean flow pore diameter. The mean flow pore diameters of the six filters are listed in Table I. The mean flow pore diameters are in the range of about 11 and 45 microns.

Gas permeability

Permeability, k is calculated from the gas flow rate using the following relation [3].

$$F = k \, [\, A / (2 \mu \, l \, p_s)] \, [p_i + p_o] \, [p_i - p_o] \quad (3)$$

where:
F = flow rate in volume at STP per unit time
A = area of the sample
μ = viscosity of gas
l = thickness of sample
p_s = standard pressure
p_i = inlet pressure
p_o = outlet pressure

The permeability of the filters are listed in Table i. Permeability varies in the wide range between about 10 and 0.5 darcies.

Inhomogeneous structure of the filter material

Scatter in the values of the largest pore diameter and mean flow pore diameter determined using samples from different parts of the same material give an indication of the extent of structural inhomogeneity of the filter material. The scatters are listed in Table II.

Table II Scatter in the values of bubble point pore diameter and mean flow pore diameter of samples taken from different parts of material.

Filter	Scatter	
	Bubble point pore diameter	Mean flow pore diameter
#1	20.8 %	4.8 %
#2	6.1 %	9.4 %
#3	5.8 %	6.3 %
#4	3.2 %	6.4 %
#5	15.6 %	7.3 %
#6	9.2 %	3.8 %

Bubble point pore diameter: The scatter in the bubble point is due to inhomogeneous distribution of large pores. In two filters (1 & 5) the variations were large (20.8 % and 15.6 %). However, the variation was much less in other filters.

Mean flow pore diameter: The variation in the mean flow pore diameter is not expected to be influenced by the scatter in the bubble point pore diameter, because the number of such large pores is usually very small. However, differences in flow distribution can change mean flow pore diameter. Scatter in the mean flow pore diameter is generally much less than the scatter in the bubble point pore diameters. However, due to inhomogeneity of a given filter, the scatter in the mean flow pore diameter could be more than that in the bubble point pore diameter as demonstrated by filter #4.

Number of pores: Samples taken from different parts of the same filter may have the same flow distribution, but the number of pores could be different. The following relation between flow rate through a dry sample and its pore size shows that dry curves can give indications of large differences in pore numbers [3].

$$F = [\pi\beta / (128\ \mu\ l\ 2p_s)]\ [p_i + p_o]\ [p_i - p_o]\ [\Sigma_i N_i D_i^4] \qquad (4)$$

where N_i is the number of pores of diameter D_i and β is a constant.

The dry curves for three different samples of filter#4 are shown in Figure 5. This filter material shows only 3.2 % scatter in the bubble point pore diameter and 6.4 % scatter in the mean flow pore diameter. However, the number of pores is much different as demonstrated by the differences between the dry curves.

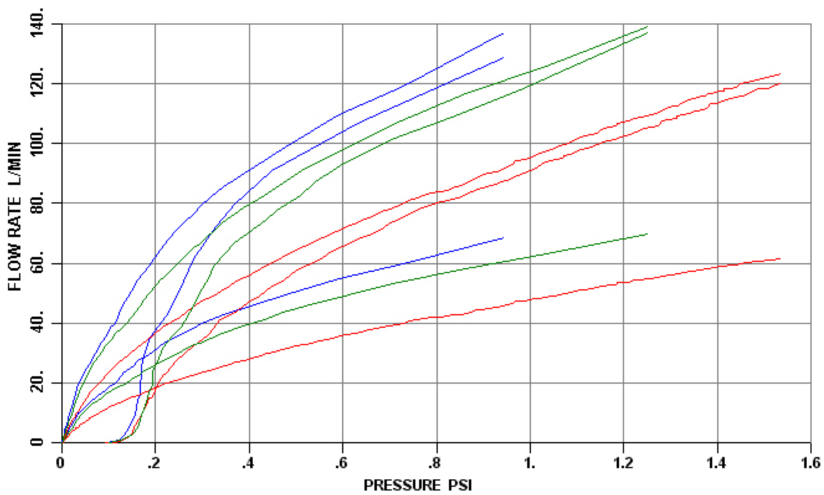

Figure 5 Data on three samples of filter #4.

Some filter materials show very little difference between number of pores at different locations as illustrated in Figure 6 for filter material #1. This filter material that shows very large scatter in the bubble point pore diameter and small scatter in mean flow pore diameter (flow distribution), also shows very small variation in pore number.

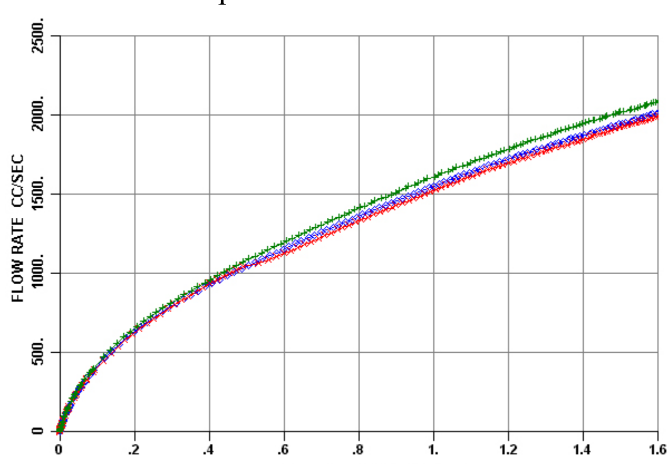

Figure 6 Dry curves of three different samples of Filter #1.

Some of the dry curves of filter material #3 were unusual. They gave indications of fiber shifting in certain regions. This structural feature also contributes to in-homogeneity in the material (Figure 7).

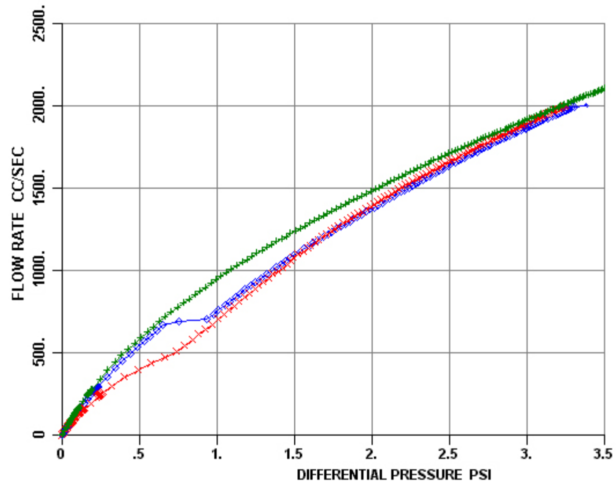

Figure 7. Some of the dry curves for filter material #3.

Composite filters

Several filter materials were combined to prepare the following composite filter media.

Composite	Constituent filters	Pore size in constituent filters
C#1	1 & 6	Large & Large
C#2	1 & 2	Large & small
C#3	1,2 & 5	Large, large & small
C#4	1,2,3,4,5 & 6	Large, small. Small. Large, Large & large

Bubble point pore diameter: Bubble points of composite filters are listed in Table III. As expected, the bubble point pore diameter is considerably reduced what ever may be the pore size in the starting material. The results of C#2, C#3 and C#4 are interesting. They show that increasing the number of layers do not have corresponding effect on the bubble point.

Table III Bubble point pore diameters of composite filters

Filters	Bubble point pore diameter, microns	Deviation from the average value
C#1 (1,6)	73.53	- 32 %
C#2 (1,2)	23.09	- 68 %
C#3 (1,2,5)	21.72	- 69 %
C#4 (1,2,3,4,5,6)	22.82	- 67 %

Mean flow pore diameter: Table IV lists the mean flow pore diameters of composite filters. As expected, the mean flow pore diameter is considerably reduced in all cases. The results obtained with C#2, C#3 and C#4 show that increasing the number of layers do not have corresponding effect on the mean flow pore diameter. Mean flow pore diameter of a composite consisting of one filter with large pores and another with small pores can be reduced by adding more filters to the composite, but the percentage reduction in the pore diameter can not be increased appreciably.

Table IV Mean flow pore diameters of composite filters

Filters	Mean flow pore diameter, microns	Deviation from the average value
C#1 (1,6)	35.00	- 18 %
C#2 (1,2)	10.38	- 66 %
C#3 (1,2,5)	9.21	- 63 %
C#4 (1,2,3,4,5,6)	7.62	- 74 %

Structural homogeneity: The composite filters were much more homogeneous than the constituent filter materials. This is brought out by the scatters (Table V) in bubble point pore diameter and mean flow pore diameter determined on samples taken from various parts of the composite filter.

Table V Scatter in bubble point and mean flow pore diameter obtained using different samples of the composite filter

Composite	% Scatter in pore diameter			
	Bubble point		Mean flow	
	Composite	Constituents	Composite	Constituents
C#1 (1,6)	5.5	20.8, 9.2	3.2	4.8, 3.8
C#3 (1,2,5)	8.3	20.8, 6.1, 15.6	4.2	4.8, 9.4, 7.3
C#4 (1,2,3,4,5,6)	11.8	20.8, 6.1, 5.8 3.2, 15.6, 9.2	3.9	4.8, 9.4, 6.3, 6.4, 7.3, 3.8

The dry curves of several samples taken from the same composite filter suggests that the number of pores changed from sample to sample, although the variation was much less than that observed in some of the constituent filter materials. Several dry curves of C#4 demonstrate this in Figure 8. The data also show that the dry and the wet curves do not meet. This feature of the curves was common to all the composite filters. It suggests that combination of filters results in creation of many small pores. Fiber slipping that was observed in one constituent filter material was not observed in composite filters.

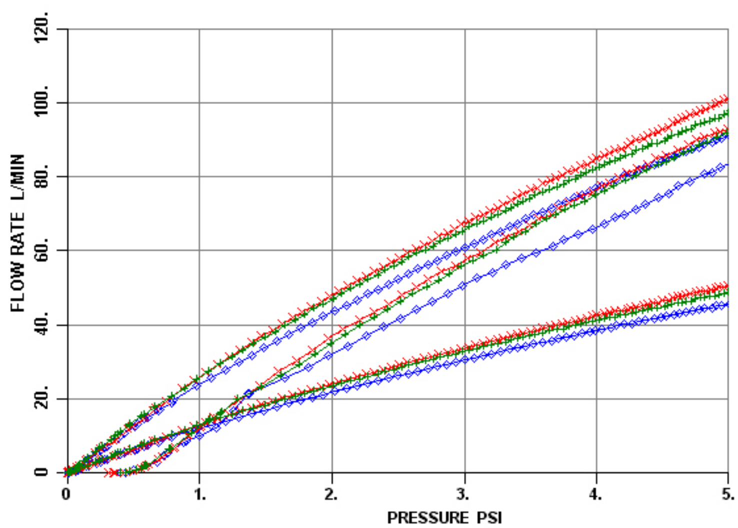

Figure 8. A number of dry and wet curves for composite filter C#4.

Permeability: The permeability of composite filter C#3 is listed below along with the permeability of constituent filters. The permeability is much higher than the lowest permeability of constituent filter materials. Thus, combination of filters reduces the pore diameter considerably below those of constituent filters while maintaining relatively high permeability. We noted earlier that combination of a large number of filters does not influence the pore diameter appreciably after the initial large change, however, permeability may be considerably reduced.

Composite, C#3	6.03 darcies
Constituent, #1	10.44 darcies
Constituent, #2	0.52 darcies
Constituent, #3	0.72 darcies

Conclusions

(1) Six filter materials having a wide range of pore diameter were investigated.
  (a) Bubble point pore diameter was between 24.29 and 120.6 microns.
  (b) Mean flow pore diameter was between 11.73 and 44.77 microns.
  (c) Permeability was between 0.52 and 10.44 darcies.

(2) Some of the materials were structurally quite in-homogeneous. Samples tested from various parts of the material showed considerable scatter.
  (a) 3.2 to 20.8% scatter in bubble point pore diameter.
  (b) 3.8 to 9.4 % scatter in mean flow pore diameter.
  (c) In some filters the number of pores varied considerably.

(3) Four composite filters were prepared combining two, three or six pre-tested filter materials.
  (a) The bubble point pore diameter and the mean flow pore diameter were considerably reduced (about 70 %).
  (b) After the large initial reduction, the magnitude of reduction was insensitive to the number of constituent filter materials.
  (c) The composite filter was structurally much more homogeneous than the constituent filter materials. The scatters were much less.
  (d) Permeability of composite filters were higher than the average permeability of constituent filter materials.

(3) Use of capillary flow porometry can provide considerable insight and flexibility in the design of composite filters.

References

1. Vibhor Gupta and A.K. Jena, Substitution of Alcohol in Porometers for Bubble Point Determination, Advances in Filtration and Separation Technology, Eds. Wallace Leung and Thad Ptak, American Filtration & Separation Society, Vol. 13b, 1999. pp. 833-844
2. A.K. Jena and K.M. Gupta, In-plane Compression Porometry of Battery Separators, J. Power Sources, Vol. 80, No. 1-2, 1999, pp. 46-52.
3. A.E. Scheidegger, The Physics of Flow Through Porous, Media, Macmillan, 1957.